Fluid Dynamics & Materials Processing

Tech Science Press

DOI: 10.32604/fdmp.2023.025843

ARTICLE

Hydrophobic Small-Molecule Polymers as High-Temperature-Resistant Inhibitors in Water-Based Drilling Fluids

Xuyang Yao[1,*], Kecheng Liu[1], Zenan Zhou[1], Jun Zhou[1], Xianbin Huang[2], Tiemei Lu[1], Yongsheng Yu[1] and He Li[2]

[1]Engineering Technology Research Institute of Xinjiang Oilfield Company, PetroChina, Karamay, 834000, China

[2]School of Petroleum Engineering, China University of Petroleum (East China), Qingdao, 266580, China

[*]Corresponding Author: Xuyang Yao. Email: yaoxuyang2019@petrochina.com.cn

Received: 02 August 2022 Accepted: 25 October 2022

ABSTRACT

Water-based drilling fluids can cause hydration of the wellbore rocks, thereby leading to instability. This study aimed to synthesize a hydrophobic small-molecule polymer (HLMP) as an inhibitor to suppress mud shale hydration. An infrared spectral method and a thermogravimetric technique were used to characterize the chemical composition of the HLMP and evaluate its heat stability. Experiments were conducted to measure the linear swelling, rolling recovery rate, and bentonite inhibition rate and evaluate accordingly the inhibition performance of the HLMP. Moreover, the HLMP was characterized through measurements of the zeta potential, particle size distribution, contact angles, and interlayer space testing. As confirmed by the results, the HLMP could successfully be synthesized with a favorable heat stability. Furthermore, favorable results were found for the inhibitory processes of the HLMP on swelling and dispersed hydration during mud shale hydration. The positively charged HLMP could be electrically neutralized with clay particles, thereby inhibiting diffusion in the double electron clay layers. The hydrophobic group in the HLMP molecular structure resulted in the formation of a hydrophobic membrane on the rock surface, enhancing the hydrophobicity of the rock. In addition, the small molecules of the HLMP could plug the spaces between the layers of bentonite crystals, thereby reducing the entry of water molecules and inhibiting shale hydration.

KEYWORDS

Water-based drilling fluids; hydrophobic polymers; shale inhibitor; temperature resistance

1 Introduction

"Drilling fluid" is a general term for the various types of circulatory fluids used in oil and gas drilling. When using water-based drilling fluids in drilling work, the liquid in the drilling fluids will create adverse conditions for wellbore rocks, especially in mud shale, which will affect the formation stability and drilling operations. This can lead to wellbore collapse, wellbore enlargement, and drill jamming, and this lack of stability is often called wellbore instability [1,2]. Wellbore instability can manifest over long periods and is a source of continuous complications in oil and gas mining. The penetration of water from drilling fluids into mud shale will lead to hydration, which is the main causative factor of wellbore collapse [3,4].

This work is licensed under a Creative Commons Attribution 4.0 International License, which permits unrestricted use, distribution, and reproduction in any medium, provided the original work is properly cited.

The use of mud shale inhibitors in drilling fluids is an important measure for suppressing dispersed hydration and swelling in mudshale or clay and stabilizing wellbores [5]. Over the years, various inhibitors including inorganic and organic salts, surfactants, and polymers have been developed [6,7]. Inorganic and organic salt inhibitors, such as potassium chloride (KCl) and potassium formate, mainly achieve the inhibitory effects through clay ion exchange to lower the water activity in the drilling fluid [8–10]. Surfactant inhibitors, typically cationic surfactants, mainly inhibit clay hydration by electrical neutralization with the clay and the compression of hydrous clay layers. Numerous polymer inhibitors operate mainly through the envelopment of clay particles to reduce reactions with water. Polyamine inhibitors have been extensively studied recently due to their excellent inhibition performance [11,12], which is mainly achieved by plugging between clay layers and reducing the entry of water molecules into the interior of the clay layers to reduce clay hydration [13,14].

The inhibitors mentioned above have unsatisfactory high-temperature resistance and limited inhibition abilities, so they cannot meet the actual drilling requirements. Some previously used high-molecular-weight polymers were found to have a large impact on the performance of drilling fluid systems, while low-molecular-weight polymers had a much smaller effect on the rheology of the drilling fluid system. Low-molecular-weight polyethylene glycols were found to exhibit some inhibitory properties, and have been used as inhibitors [15,16]. Zhao et al. [17] prepared a low-molecular-weight amphoteric terpolymer by free radical polymerization, and the polymer effectively inhibited shale hydration. In addition, a variety of low-molecular-weight amine-based polymers were found to be effective shale inhibitors, including polyamine acid, poly-hydroxylated alkyl ammonium salt, polyethoxylated diamines, and dendritic amines [18]. Bai et al. [19] prepared an amino polyether and evaluated its inhibitory properties; the results showed that the inhibitor had better inhibition performance than other conventional inhibitors. Organic-cation-based shale inhibitors have been proposed for use with water-based drilling fluids to inhibit the hydration swelling of mud shale in water-sensitive shale formations. A hydrophobic shale inhibitor with low-molecular-weight cations was developed, which adsorbed on the surface of rocks, changed the wettability of the rock through the hydrophobic groups in the molecular structure, and reduced the probability of water molecules invading the clay layer.

In this study, acrylamide (AM), (3-acrylamide propyl) trimethylammonium chloride (ATAC), and butyl methacrylate (BMA) were combined to form a low-molecular-weight ternary copolymer. Inhibition was evaluated by testing the linear swelling, rolling recovery rate, and bentonite inhibition rate. Zeta potential, particle size, particle size distribution, contact angle, and interlayer space measurements, as well as scanning electron microscopy (SEM) observations, were obtained to study the mechanism of this hydrophobic low-molecular-weight polymer (HLMP). This study may guide the future development of hydrophobic polymer inhibitors.

2 Materials and Methods

2.1 Materials

Acrylamide (AM, 99.0 wt%), (3-acrylamide propyl) trimethylammonium chloride (ATAC, 75.0 wt%), butyl methacrylate (BMA, 95.0 wt%), ethanol (99.9 wt%), potassium chloride (99.5 wt%), and benzoyl peroxide (BPO, 99.0 wt%) were purchased from Aladdin Chemical Reagents (Shanghai, China). Polyetheramine D230 (PAD230) was purchased from Shanghai Juxin Chemical (China). Bentonite and rocks were provided by the Xinjiang Oilfield Company (China). The detailed mineralogical composition of the shale is presented in Table 1.

Table 1: Mineralogical composition of the shale

Component	wt%
Plagioclase	24.1
Potassium feldspar	1.5
Calcite	2.4
Siderite	1.2
Quartz	24.2
Chlorite	3.8
Illite	14.4
Kaolinite	11.1
Halite	4.5
Illite/smectite mixed layer	12.8

2.2 Preparation of HLMP

First, 100 mL of ethanol was added to a 250 ml three-neck flask and then stirred after the addition of 3 g of AM. After the AM was completely dissolved, 1.8 g of ATAC and 0.2 g of BMA were added in turn and stirred well to allow for complete dissolution. Subsequently, an oil bath pot was used to heat up the reaction system to 80°C, and nitrogen was introduced into the flask for 30 min to remove oxygen. Then, 0.1 g of BPO was added to trigger the reaction. After 4 h (a full reaction), a large volume of ethanol was used to precipitate the product of interest. The product was dried at 70°C and crushed at 25 ± 2°C to produce a powdered polymer, which was the HLMP. The chemical reaction equation of HLMP synthesis is shown in Fig. 1.

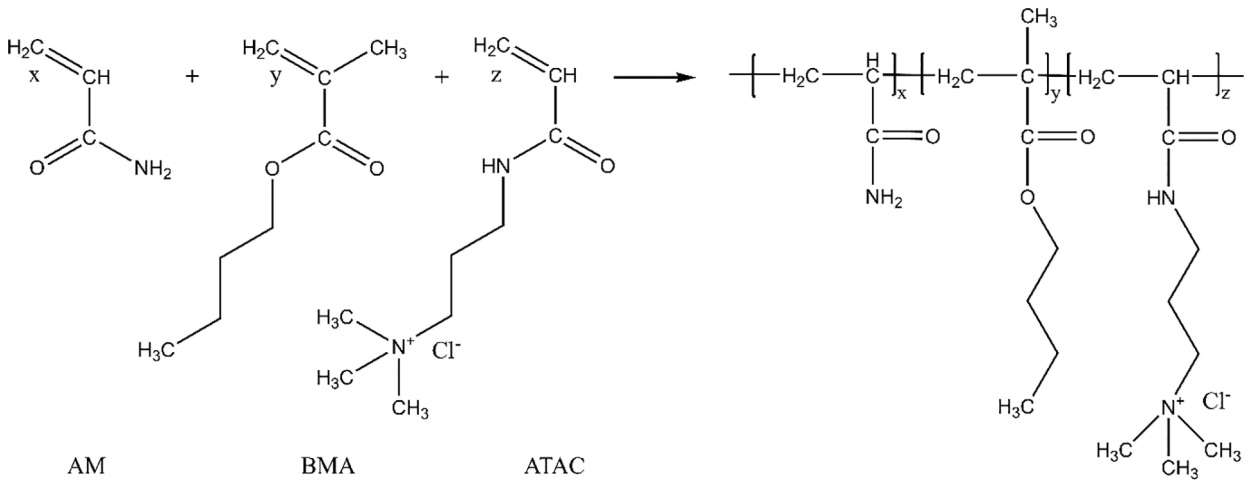

Figure 1: The chemical reaction equation of HLMP synthesis

2.3 Characterization

The purified HLMP was freeze-dried and then ground into a powder, and its infrared spectrum was obtained by an Antaris II Fourier Transform Near-Infrared Spectrometer (USA) using the potassium bromide tableting method. Under a nitrogen atmosphere, the thermogravimetric curves of the HLMP at

40°C–700°C were obtained using an HTG-2 Thermogravimetric Analyzer (Mettler, Switzerland), with a heating rate of 10 °C/min.

2.4 Inhibition Performance of HLMP

2.4.1 Linear Swelling Test

A sample of bentonite was oven-dried to a constant weight. An electronic scale was used to accurately weigh 10.0 g of bentonite, which was loaded into a core mold and pressurized to 10 MPa using a hydraulic press. The stress was relieved after 10 min, and the rock samples were obtained. The rock samples were loaded into a CPZ-II dual-channel linear swelling tester and soaked in different inhibitor solutions. The expansion of the rock samples was recorded, and the experiment was completed after 16 h.

2.4.2 Hot-Rolling Recovery Test

Red mud shale selected from an outcrop in Songlinzhen, Sichuan, China, was crushed into rock chip sieves with mesh numbers of 6–10 and dried to a constant weight in a drying box. Five 50 g portions of rock chips were placed in separate aging tanks. An inhibitor solution (350 mL) with a mass friction of 1.0% was prepared and added to the aging tanks containing the rock chips and aged at 120°C for 16 h. After aging was complete, the obtained samples were cooled to 25 ± 2°C, rinsed several times with tap water, and passed through a standard 40-mesh sieve. The chips that remained on the sieve were dried at 100°C to a constant weight in the drying box, and the mass value was recorded as M. The rolling recovery rate was calculated by:

$$R = \frac{M_2}{M_1} \times 100\%, \tag{1}$$

where R is the rolling recovery rate (%), M_1 is the initial mass of the rock chips, and M_2 is the mass of the remained chips (g).

2.4.3 Relative Inhibition Rate Test

Five samples of 350 mL of aqueous solutions containing 1.0 wt% HLMP were prepared using goblets, with 350 mL of water used as the blank control group. Next, 35 g of bentonite was slowly added to each HLMP sample and stirred at a speed of 5000 rpm for 20 min, sealed, and left at 25 ± 2°C for 16 h. After that, the obtained HLMP–bentonite system was stirred for 20 min at 5000 rpm, and viscosity readings were obtained at 100 rpm (Φ100) using a 6-speed rotary viscometer. After measurement, the HLMP–bentonite system was again loaded into the aging tanks and aged at different temperatures for 16 h. Following that, the system was cooled to 25 ± 2°C and stirred at 5000 rpm for 20 min. The Φ100 viscosity was measured again using the viscometer. The following equation was used to calculate the relative inhibition rate after aging:

$$I = \frac{\phi_1 - \phi_2}{\phi_2} \times 100\%, \tag{2}$$

where I is the relative inhibition rate (%), Φ_1 is the stable Φ100 viscosity reading for the pure bentonite slurry aged at different temperatures for 16 h, and Φ_2 is the stable Φ100 viscosity reading of the HLMP–bentonite system after aging for 16 h.

2.5 Mechanism Analysis

2.5.1 Zeta Potential Measurement

A 4.0 wt% bentonite slurry was prepared with 16 g of bentonite dispersed in 400 mL of water, which was left to stand at 25 ± 2°C for 24 h. Different concentrations (0, 0.5, 1.0, 1.5, and 2 wt%) of the HLMP inhibitor were added to 100 mL of the prepared base slurry and stirred for 24 h to allow the HLMP to

fully adsorb on the clay surface. Subsequently, a Zetasizer Nano ZS (Malvern Instruments, UK) was used to test for changes in the electrical potential of the clay.

2.5.2 Particle Size Distribution Test

After different concentrations of HLMP were added to the bentonite slurry prepared as described above, they were poured into an aging tank and sealed. The aging tank was placed into a roller heating furnace and aged at 150°C for 16 h. After cooling, the change in the particle size of the bentonite following the addition of HLMP was measured using a Mastersizer 3000E Particle Size Analyzer (Malvern, UK).

2.5.3 Contact Angle Measurement

Cut chips were placed in different aging tanks, and then aqueous HLMP solutions with different concentrations (0, 0.5, 1.0, 1.5, and 2 wt%) were added. After aging at 150°C for 16 h, the rock chips were removed. After drying at ambient temperature, changes in the contact angle of the rock chips were tested using a contact angle measuring instrument (OCA 255, Shimadzu, Japan).

2.5.4 Interlayer Space Measurement

HLMP was added to 100 mL of the prepared bentonite slurry and aged at 150°C for 16 h. After aging, the slurry was centrifuged for 5 min at 8000 rpm. After centrifugation, a layer of sediment was removed, dried at 105°C, ground into a powder, and the change in the grain spacing of the bentonite was measured using X-ray diffraction (D8 DISCOVER, Bruker, Germany).

2.5.5 SEM Analysis

The surface morphology of the shale before and after HLMP treatment was observed by scanning electron microscopy (Nova NanoSEM 450, USA). The treatment process of the shale was the same as for contact angle measurement.

3 Results and Discussion

3.1 Fourier-Transform Infrared Spectroscopy (FTIR)

Fig. 2 shows the FTIR spectra of the HLMP shale inhibitor, where the peak at 2950 cm^{-1} was the stretching vibration peak of CH_2 in the main polymerization chain, and the peak at 1673 cm^{-1} was the stretching vibration peak of the amide bonds (C=O) in the AM and ATAC. The peak at 3370 cm^{-1} was the stretching vibration peak of the amide bonds (N-H) in the AM and ATAC, and the peak at 1420 cm^{-1} was the C-N stretching peak of the amide bonds in the AM and ATAC. The characteristic absorption peak of the quaternary ammonium salt in the ATAC appeared at 1451 cm^{-1}. The C=O stretching vibration peak of the ester groups in the BMA appeared at 1725 cm^{-1}, while the C-O stretching vibration peak of the ester groups in the BMA appeared at 1207 cm^{-1}. The characterization results showed that the synthesized product contained a functional group that was unique to the monomers, and all were fully reacted.

3.2 Thermogravimetric Analysis (TGA)

The thermal stability of the synthesized products was studied using an HTG-2 thermogravimetric synchronization analyzer, and the results are shown in Fig. 3. The HLMP shale inhibitor experienced a small amount of weight loss before 136°C, which was mainly due to the volatilization of a small quantity of free water molecules in the sample. Between 136°C and 263°C, the bonded water absorbed by the strong hydrophilic amide groups in the specimen molecules began to volatize due to heating. From 267°C to 336°C, the thermogravimetric curve fell sharply due to the disintegration and volatilization of amide groups in the molecular structure. At the stage between 336°C and 378°C, the ester groups in the copolymer molecules started to decompose rapidly, and the main and side chains of the copolymer molecule began to break. This showed that the thermal stability of the polymerization products was favorable.

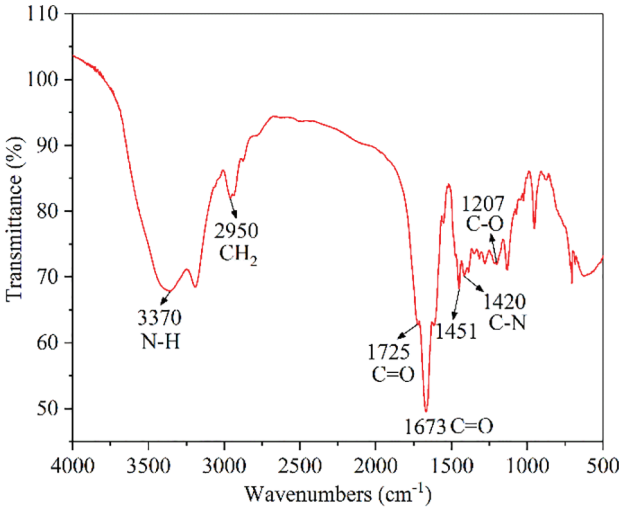

Figure 2: FTIR spectra of the HLMP shale inhibitor

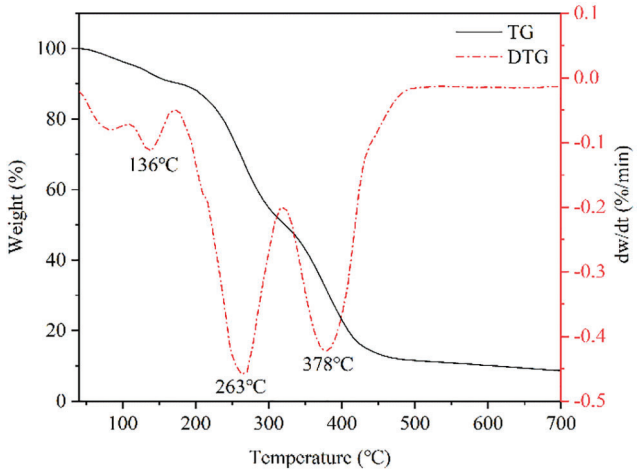

Figure 3: Thermogravimetric curve of the HLMP shale inhibitor

3.3 Inhibition Performances of HLMP

3.3.1 Linear Swelling Test

The effects of different inhibitors on the expansion of bentonite rock samples are shown in Fig. 4. The largest swelling of the bentonite rock samples occurred in water (7.85 mm), suggesting that the rock samples in water underwent significant hydration-related expansion. Compared with the expansion in water, the expansions of the rock samples in 5.0 wt% KCl, 1.0 wt% PAD230, 0.5 wt% HLMP, and 1.0 wt% HLMP were reduced to 5.64, 4.47, 2.68, and 2.12 mm, respectively. Therefore, the 1.0 wt% HLMP had the best performance in terms of inhibiting the expansion of the rock samples, which demonstrated the effectiveness of the HLMP at inhibiting hydration-related expansion of the bentonite rock.

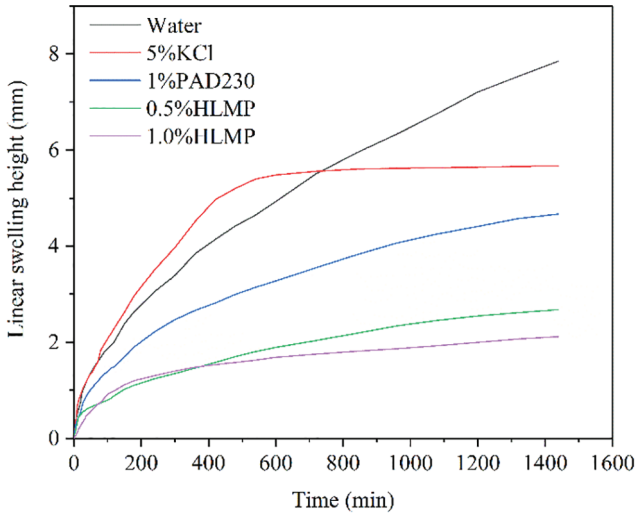

Figure 4: Linear expansion results of the HLMP

3.3.2 Hot-Rolling Recovery Test

The effects of different inhibitors on the rolling recovery rate of red mud shale rock chips are shown in Fig. 5. This indicated that after aging at 120°C, the rolling recovery rate of the rock chips was the smallest in water at only 5.8 wt%, which suggested that significant dispersed hydration occurred within these rock chips. The rolling recovery rates of rock chips in 5.0 wt% KCl, 1.0 wt% PAD230, 0.5 wt% HLMP, and 1.0 wt% HLMP were 46.8, 56.7, 76.9, and 83.9 wt%, respectively. The rolling recovery rate was the highest for the rock chips in 1.0 wt% HLMP, with a value of 83.9 wt%, indicating that the HLMP had more favorable inhibition of the hydration dispersion properties of the rock chips.

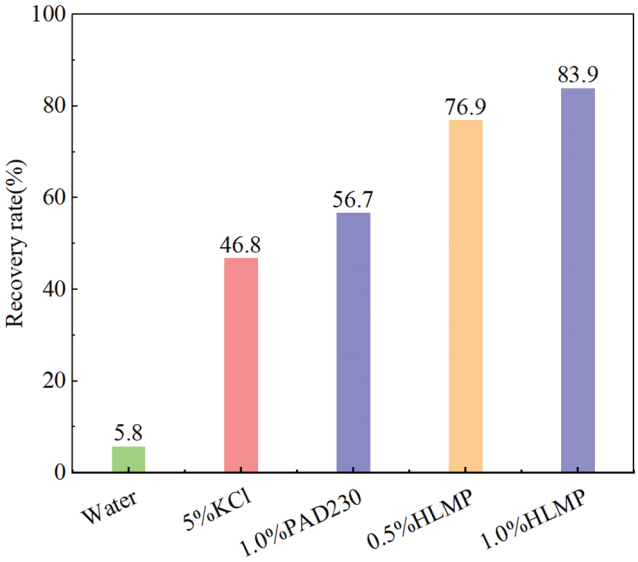

Figure 5: Shale recovery results of HLMP

3.3.3 Relative Inhibition Rate Test

The performance results of 1.0 wt% HLMP on the hydration of the bentonite slurry after aging for 16 h at different temperatures are shown in Fig. 6, which indicated that after 16 h of aging at 30°C, 60°C, 90°C, 120°C, and 150°C, the inhibition rates were 88.9%, 87.6%, 85.4%, 87.2%, and 92.3%, respectively, which all exceeded 85%. This meant that HLMP significantly inhibited hydration in the bentonite slurry. The HLMP aged at different temperatures all exhibited significant inhibitive performance, indicating that the HLMP had excellent heat resistance.

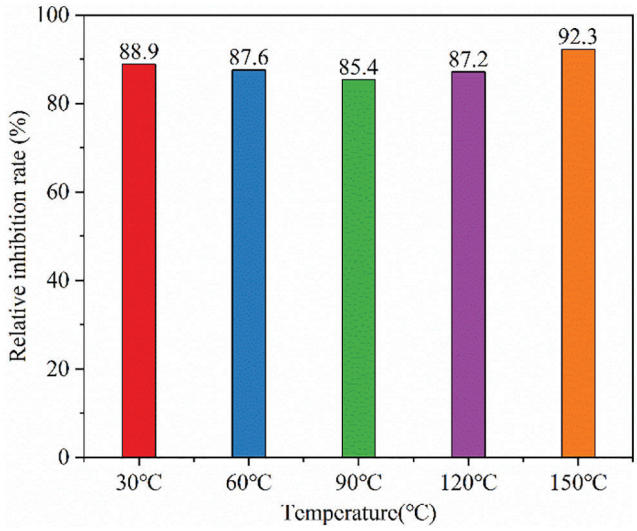

Figure 6: Inhibition rates of the HLMP on bentonite under different temperatures

3.4 Mechanism Analysis

3.4.1 Zeta Potential Measurements

The influence of the HLMP concentration on the electrical potential of bentonite is shown in Fig. 7, where the zeta potential of the clay particles was low and the tendency for dispersion was high. The zeta potential of the bentonite gradually increased with an increase in HLMP concentration. This change was due to the neutralization of the negatively charged clay particles with the positively charged HLMP. The changes in the zeta potential of bentonite indicated that the HLMP adsorbed onto the clay particles, thus changing the electrostatic forces and inhibiting the dispersion of the clay particles.

3.4.2 Particle Size Distribution Tests

Fig. 8 shows the influence of the HLMP concentration on the particle distribution in bentonite. The particle size significantly increased with increasing concentration of the HLMP. The median particle size of untreated bentonite in water was 8.2 μm. The median particle sizes of bentonite increased to 87.8, 103.1, 120.7, and 132.2 μm when the HLMP concentrations increased to 0.5, 1.0, 1.5, and 2.0 wt%, respectively. The significant increase in particle size of bentonite indicated that HLMP effectively inhibited the dispersion of water in bentonite.

3.4.3 Contact Angle Measurements

The influence of HLMP concentration on the contact angle of the rock is shown in Fig. 9. The original rock contact angle was only 12°, indicating that the surface was hydrophilic. In the rock treated with HLMP, the contact angle gradually increased as the HLMP concentration increased. After treatment with 0.5, 1.0, 1.5, and 2.0 wt% HLMP, the contact angle increased to 78°, 91°, 102°, and 105°, respectively. The

changes in the contact angle, and hence rock wettability, were the result of a thin hydrophobic layer that formed due to the tight arrangement of the outward-facing long hydrophobic chains in the molecular structure of the HLMP. Changes in the wettability made the rock less susceptible to hydration.

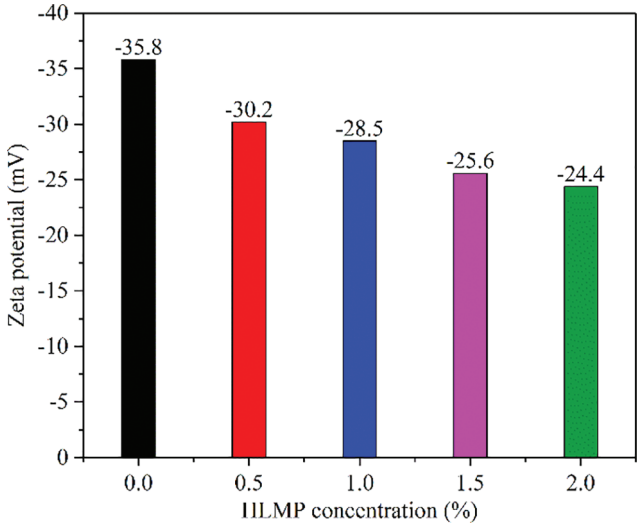

Figure 7: Effect of HLMP concentration on the zeta potential of bentonite

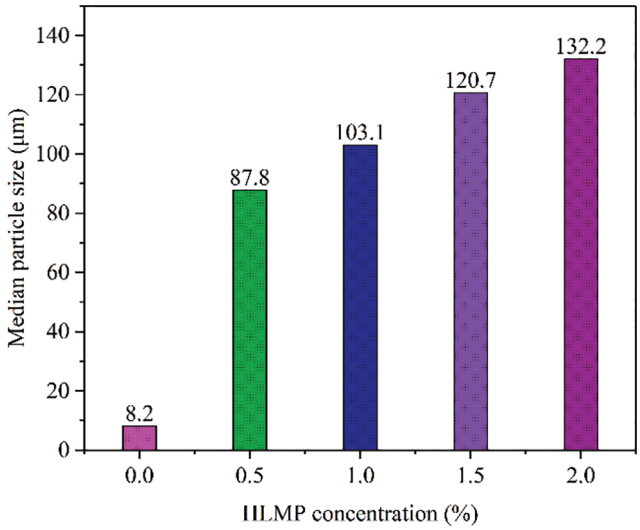

Figure 8: Effect of HLMP concentration on the median particle size of bentonite

3.4.4 Interlayer Space Measurements

Fig. 10 shows the interlayer spacing of dry bentonite after treatment with different concentrations of HLMP. The interlayer spacing of the untreated bentonite was 1.223 nm. After treatment with HLMP concentrations of 0.5, 1.0, 1.5, and 2.0 wt%, the interlayer spacing increased to 1.335, 1.342, 1.363, and 1.368 nm, respectively. The increase in the crystal layer spacing indicated that the HLMP molecules could be inserted between the bentonite layers, thus reducing bentonite hydration.

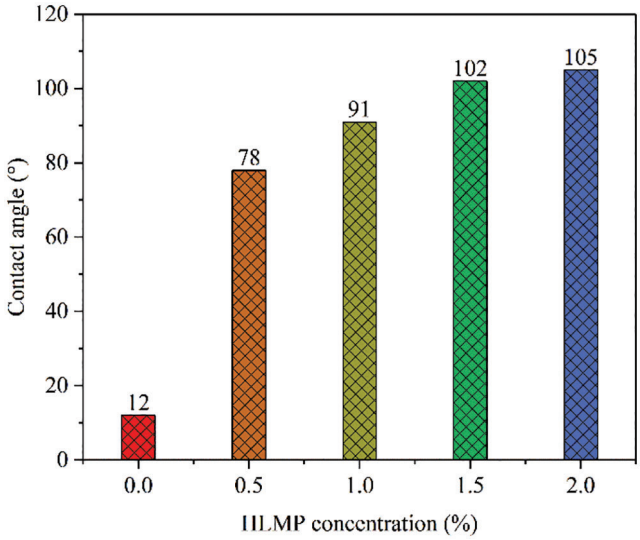

Figure 9: Effect of HLMP concentration on the contact angle of the rock

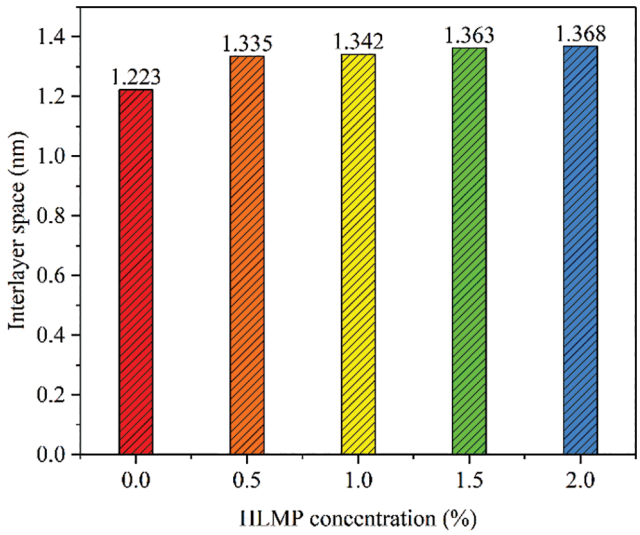

Figure 10: Interlayer spaces of bentonite treated with HLMP at various concentrations

3.4.5 SEM Analysis

SEM was used to analyze the surface morphology of the shale, and the results are shown in Fig. 11. As shown in Fig. 11a, the original shale surface was loose and porous, which provided a channel for water to enter the interior of the shale. After HLMP treatment, there was a significant difference in the observed shale surface, as shown in Fig. 11b. The HLMP-treated shale surface became denser and less porous due to HLMP adsorption and a hydrophobic membrane formed on the shale surface, which prevented the invasion of water into the shale.

The schematic diagram of the inhibition mechanism of HLMP is shown in Fig. 12. The untreated shale underwent hydration when it made contact with the water in the drilling fluids. By contrast, the hydration of shale treated with HLMP was inhibited. The HLMP adsorbed on the surface of the shale and formed a hydrophobic membrane structure with alkyl chains pointing outwards. Therefore, the wettability of the shale was altered and the intrusion of water into the shale was inhibited due to the hydrophobic membrane. The inhibitory effect was the result of the HLMP hydrophobic membrane.

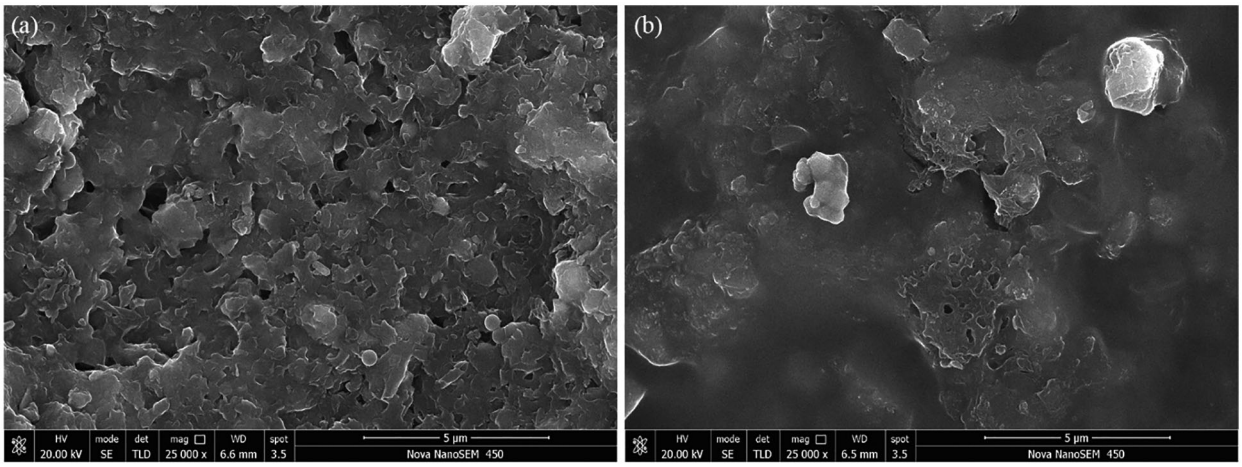

Figure 11: SEM images of the shale before (a) and after (b) 1.0 wt% HLMP treatment

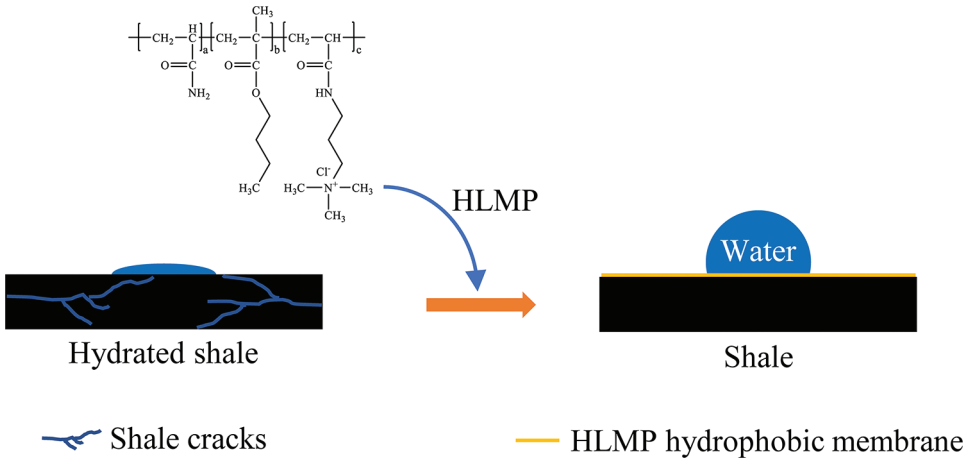

Figure 12: Schematic diagram showing the inhibition mechanism of HLMP

4 Conclusions

In this paper, a hydrophobic ternary copolymer with a low molecular weight, HLMP, was successfully prepared/synthesized. The experimental results indicated that the HLMP had an excellent inhibitory effect and could effectively inhibit hydration-induced swelling and dispersed hydration in shale and clay. The synthesized HLMP also had excellent application potential. In this work, we only conducted experiments to evaluate the inhibitory properties of HLMP at 120°C. The study of its heat resistance should be conducted in future work.

Acknowledgement: The authors thank the Integration and Testing of Safe and Fast Drilling and Completion Technologies for Complex Ultra-Deep Wells (2020F-46) and Major Technology Field Test of Joint-Stock Company (Drilling and Production Engineering).

Funding Statement: The work is supported by the Integration and Testing of Safe and Fast Drilling and Completion Technologies for Complex Ultra-Deep Wells (2020F-46) and Major Technology Field Test of Joint-Stock Company (Drilling and Production Engineering). Xuyang received the grant.

Conflicts of Interest: The authors declare that they have no conflicts of interest to report regarding the present study.

References

1. Huang, X., Sun, J., Li, H., Wang, R., Lv, K. et al. (2022). Fabrication of a hydrophobic hierarchical surface on shale using modified nano-SiO_2 for strengthening the wellbore wall in drilling engineering. *Engineering, 11,* 101–110. https://doi.org/10.1016/j.eng.2021.05.021
2. Li, H., Sun, J., Lv, K., Huang, X., Zhang, P. et al. (2022). Wettability alteration to maintain wellbore stability of shale formation using hydrophobic nanoparticles. *Colloids and Surfaces A: Physicochemical and Engineering Aspects, 635,* 128015. https://doi.org/10.1016/j.colsurfa.2021.128015
3. Peng, B., Luo, P., Guo, W., Yuan, Q. (2013). Structure-property relationship of polyetheramines as clay-swelling inhibitors in water-based drilling fluids. *Journal of Applied Polymer Science, 129(3),* 1074–1079. https://doi.org/10.1002/app.38784
4. An, Y., Jiang, G., Ren, Y., Zhang, L., Qi, Y. et al. (2015). An environmental friendly and biodegradable shale inhibitor based on chitosan quaternary ammonium salt. *Journal of Petroleum Science and Engineering, 135,* 253–260. https://doi.org/10.1016/j.petrol.2015.09.005
5. Ni, X., Jiang, G., Li, Y., Yang, L., Li, W. et al. (2019). Synthesis of superhydrophobic nanofluids as shale inhibitor and study of the inhibition mechanism. *Applied Surface Science, 484,* 957–965. https://doi.org/10.1016/j.apsusc.2019.04.167
6. de Carvalho Balaban, R., Vidal, E. L. F., Borges, M. R. (2015). Design of experiments to evaluate clay swelling inhibition by different combinations of organic compounds and inorganic salts for application in water base drilling fluids. *Applied Clay Science, 105,* 124–130.
7. Ferreira, C. C., Teixeira, G. T., Lachter, E. R., Nascimento, R. S. V. (2016). Partially hydrophobized hyperbranched polyglycerols as non-ionic reactive shale inhibitors for water-based drilling fluids. *Applied Clay Science, 132,* 122–132. https://doi.org/10.1016/j.clay.2016.05.025
8. Chu, Q., Lin, L., Su, J. (2020). Amidocyanogen silanol as a high-temperature-resistant shale inhibitor in water-based drilling fluid. *Applied Clay Science, 184,* 105396. https://doi.org/10.1016/j.clay.2019.105396
9. Jiang, G., Qi, Y., An, Y., Huang, X., Ren, Y. (2016). Polyethyleneimine as shale inhibitor in drilling fluid. *Applied Clay Science, 127,* 70–77.
10. Gholami, R., Elochukwu, H., Fakhari, N., Sarmadivaleh, M. (2018). A review on borehole instability in active shale formations: Interactions, mechanisms and inhibitors. *Earth-Science Reviews, 177,* 2–13. https://doi.org/10.1016/j.earscirev.2017.11.002
11. Chen, G., Yan, J., Lili, L., Zhang, J., Gu, X. et al. (2017). Preparation and performance of amine-tartaric salt as potential clay swelling inhibitor. *Applied Clay Science, 138,* 12–16. https://doi.org/10.1016/j.clay.2016.12.039
12. Shadizadeh, S. R., Moslemizadeh, A., Dezaki, A. S. (2015). A novel nonionic surfactant for inhibiting shale hydration. *Applied Clay Science, 118,* 74–86. https://doi.org/10.1016/j.clay.2015.09.006
13. Zhong, H., Qiu, Z., Sun, D., Zhang, D., Huang, W. (2015). Inhibitive properties comparison of different polyetheramines in water-based drilling fluid. *Journal of Natural Gas Science and Engineering, 26,* 99–107. https://doi.org/10.1016/j.jngse.2015.05.029
14. Zhong, H., Qiu, Z., Tang, Z., Zhang, X., Xu, J. et al. (2016). Study of 4, 4′-methylenebis-cyclohexanamine as a high temperature-resistant shale inhibitor. *Journal of Materials Science, 51(16),* 7585–7597. https://doi.org/10.1007/s10853-016-0037-y
15. de Souza, C. E. C., Lima, A. S., Nascimento, R. S. V. (2010). Hydrophobically modified poly(ethylene glycol) as reactive clays inhibitor additive in water-based drilling fluids. *Journal of Applied Polymer Science, 117(2),* 857–864. https://doi.org/10.1002/app.31318
16. Bland, R., Smith, G. L., Eagark, P., van Oort, E., Dharma, N. (1996). Low salinity polyglycol water-based drilling fluids as alternatives to oil-based muds. In: *SPE/IADC Asia Pacific drilling technology*, pp. 273–285. Kuala Lumpur, Malaysia.

17. Zhao, X., Qiu, Z., Zhang, Y., Zhong, H., Huang, W. et al. (2017). Zwitterionic polymer P(AM-DMC-AMPS) as a low-molecular-weight encapsulator in deepwater drilling fluid. *Applied Sciences, 7(6),* 594. https://doi.org/10.3390/app7060594
18. Ahmed, H. M., Kamal, M. S., Al-Harthi, M. (2019). Polymeric and low molecular weight shale inhibitors: A review. *Fuel, 251,* 187–217. https://doi.org/10.1016/j.fuel.2019.04.038
19. Bai, X., Zhang, X., Koutsos, V., Fu, Z., Ning, T. et al. (2019). Preparation and evaluation of amine terminated polyether shale inhibitor for water-based drilling fluid. *SN Applied Sciences, 1(1),* 1–9. https://doi.org/10.1007/s42452-018-0112-x